

Fabrication and Microstructure of Sialon-bonded Silicon Carbide

Ke Changming,^{a*} J.-J. Edrees^b and A. Hendry^b

^aDepartment of Materials Science and Engineering, Wuhan Iron and Steel University, Wuhan, People's Republic of China

^bMetallurgy and Engineering Materials Group, University of Strathclyde, Glasgow, UK

(Received 14 July 1998; accepted 10 January 1999)

Abstract

The sintering behaviour of ceramic-matrix composites consisting of a sialon matrix and silicon carbide particulate reinforcement has been studied in order to elucidate the densification behaviour and the formation of the microstructure. The materials are produced from a mixture of clay, silicon nitride and yttria sintering additive mixed with 60% of silicon carbide grit. The results lead to a description of the mechanism of phase formation which consists of the following steps:

1. Decomposition of china clay and formation of mullite and silica on heating.
2. Formation of liquid phase from these reaction products, together with excess silica from silicon carbide and yttria sintering additive.
3. Dissolution of silicon nitride in the liquid and precipitation of sialon X and O' phases.
4. Formation of a high-yttrium, nitrogen glass on cooling.

Composites of this kind with porosity of about 14% and zero linear shrinkage on firing, due to the rigid skeleton of carbide particles, are promising candidate materials for high-temperature applications where the microstructure offers the prospect of superior high-temperature strength through the continuous interlocking texture of the X-phase and O'-silicon oxynitride crystalline phases, the carbide skeleton and the high viscosity yttrium-nitrogen glass matrix. © 1999 Elsevier Science Limited. All rights reserved

Keywords: sintering, composites, microstructure-final, sialon, SiC.

1 Introduction

Considerable effort has been devoted to the development of engineering ceramics and ceramic-matrix composites for high-temperature applications and much of this work has been directed at silicon nitride systems including sialon solid solutions. The principal nitride phases can be formed in a number of ways and the method used in practice is determined as much by economic as by technical considerations. In the case of large components such as gas-fired radiant heater tubes as shown in Fig. 1, the reaction of silicon nitride with clay, provides from the latter material, the degree of plasticity required for green forming and from the former a source of nitrogen to produce sialon *in situ* at sintering temperature. Silicon nitride reacts with clay in the presence of a sintering additive to precipitate a needle-like structure of sialon and this has been demonstrated in previous work by the present authors,¹ on bonding systems for sialon composites in which calcium oxide was used as the sintering additive. The type and amount of the sintering additive have major influences on the sintering temperature and hence on the rate of densification. Moreover they have an effect on the morphology of the grains and the behaviour of the grain boundaries which in turn influence the high-temperature mechanical properties of the composite material. It is well known that the sintering additives react with silica and alumina present in the matrix material formulation to form liquid at the sintering temperature and if the amount of liquid is high enough and the viscosity at sintering temperature is sufficiently low then effective liquid-phase sintering will take place.^{2–7} The temperature of formation of the initial liquid phase in a given oxide system is also found to be affected by nitrogen.² That is, nitrogen as an additional component lowers the eutectic temperature of the oxide system and this has been shown in previous work to occur

*To whom correspondence should be addressed.

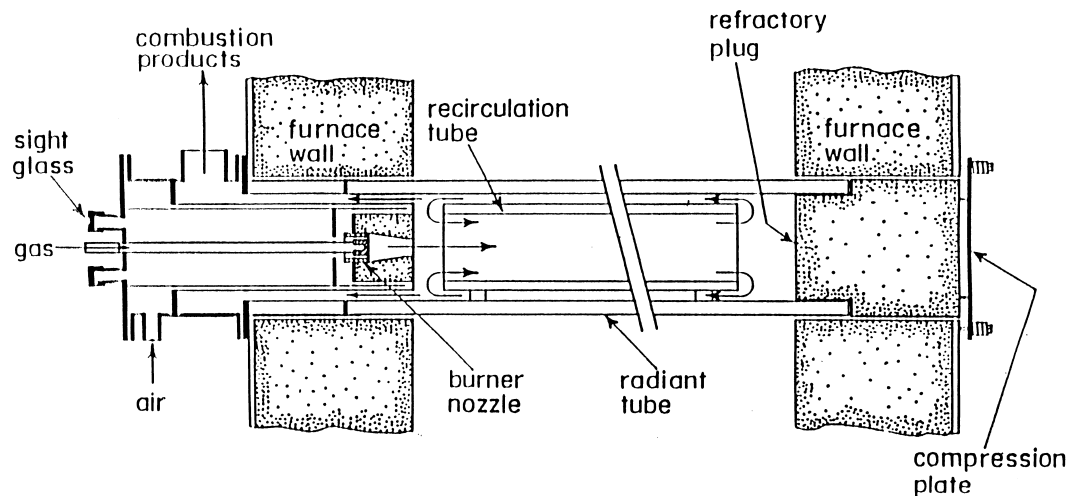


Fig. 1. Schematic representation of the design of a gas-fired radiant heater tube in which the outer tube is fabricated from ceramic-matrix composite materials

in calcium oxide containing systems.¹ It has also been shown that softening temperature, viscosity (and consequently the beginning of sintering), rate of densification, and shrinkage can be changed by the addition of different metal oxides,³⁻⁵ and that the type and amount of sintering additive have marked effects on sialon grain morphology and grain growth.^{6,7}

Most of the previous work on sialon systems has been directed at the formation of monolithic sialon ceramics but similar principles apply to formation of sialon-matrix composites.¹ The behaviour of such systems during densification and a sintering model based on a rule-of-mixtures approach have been reported^{8,9} for calcium oxide as the densification additive. However, such additives give a relatively low-temperature of liquid phase formation and consequently the maximum temperature of use is limited to about 1200°C. The grain boundary amorphous phase in certain systems can be recrystallised on heat treatment resulting in improved high-temperature mechanical behaviour and although this is of limited value with calcium oxide additive it is found to be particularly effective when yttria is the sintering additive.¹⁰ Since the eutectic temperatures in the silica-alumina-yttria system are also considerably higher than those in the corresponding calcium phase diagrams¹¹ the use of yttria as an additive offers the promise of superior ceramic composite matrices. Similarly, it has recently been shown¹² that viscosity of the matrix has a pronounced effect on high-temperature viscoelastic creep of ceramic matrix composites containing particles.

In the present work, the approach of using silicon nitride and china clay as starting materials to give sialon and introducing yttrium oxide as sintering additive was employed to produce a high-temperature

matrix in which silicon carbide aggregate was distributed to give a superior ceramic-matrix composite. The materials specification for the tubular components illustrated in Fig. 1 can be summarised as requiring to provide:

1. Zero linear shrinkage on sintering (to preserve dimensional tolerance).
2. Zero gas permeability in service (the requirement for closed porosity).
3. Adequate mechanical strength (creep resistance in service).

These properties are set by the tube manufacturers and it is the aim of the present work to design microstructures to satisfy these requirements. Densification, phase composition and microstructure of the resulting materials were studied. The compositions chosen for the sialon matrix are not the usual β' -sialon materials but are based on silicon oxynitride solid solutions (O') and X-phase sialon. These were chosen, as the typical morphology of these phases is acicular or plate-like and are considered to offer superior room-temperature toughness and high-temperature strength. The mechanical properties are however not reported here as the specific aim of this study was to characterise fully the sintering reactions in order to control shrinkage during firing of the composites.

2 Experimental Methods

The formulation of the matrix composition is based on the fact that silicon nitride, china clay and yttria react at sintering temperature to form a nitrogen-rich liquid from which sialon phases form and sintering occurs. Commercial silicon nitride

(Starck LC 10) was mixed with clay (ECC Ltd Grade D) and yttrium oxide (Analar Grade) in appropriate proportions as given below (wt%);

- Composition 1: 36% silicon nitride + 54% china clay + 10% yttria (equivalent to 40% silicon nitride in clay; Fig. 2)
- Composition 2: 27% silicon nitride + 63% china clay + 10% yttria (equivalent to 30% silicon nitride in clay; Fig. 2)
- Composition 3: 18% silicon nitride + 72% china clay + 10% yttria (equivalent to 20% silicon nitride in clay; Fig. 2)

Figure 2(a) gives the composition on the sialon behaviour diagram of the matrix powder mixes (expressed as silicon nitride and kaolinite). The corresponding compositions in the $\text{SiO}_2\text{-Al}_2\text{O}_3\text{-Y}_2\text{O}_3$ which form the initial (oxide) sintering liquids are shown in Fig. 2(b) and the yttrium is accommodated in the intergranular (amorphous,

oxynitride) phase after sintering. The powders were mixed with 5% methylcellulose binder and pelleted by uniaxial pressing at 75 MPa followed by isostatic pressing at 250 MPa to give cylindrical compacts of 30 mm diameter and 10 mm height. Matrix compositions without carbide aggregate were prepared in this way and the optimum sintering temperature determined in a series of experiments at 1500, 1530, 1550, and 1580°C for 4 h.

Green fabrication of the composites follows the same process to prepare the matrix, to which is then added silicon carbide aggregate in the proportion 40% matrix to 60% aggregate. The carbide has a range of mean particle sizes from fines (10 μm) to 2 mm and is of commercial refractory grade. Three compositions of matrix and carbide in the 40:60 ratio were prepared by wet milling in propan-2-ol with alumina balls and subsequently dried. The dried mix was also dry milled for 10 min immediately prior to compaction. The composite compacts were fired at the optimised matrix sintering temperature. By using a protective powder bed in all sintering experiments, weight losses were negligible indicating that there is no appreciable change from the starting compositions.

Measurements were made of the bulk density and porosity of the fired materials using water immersion, the microstructure was examined by optical and scanning electron microscopy and the phases present were identified by X-ray diffraction.

3 Results and Discussion

3.1 Densification of matrix mixes and formation of sialon phases

For the matrix quinary compositions used and shown in Fig. 2, the eutectic temperature is about 1470°C^{2,13} and is decreased further by the presence of yttria¹¹ and so for the range of temperatures used to investigate matrix sintering, densification occurs by a liquid-phase process. The effect of temperature on the final sintered density after 4 h in nitrogen gas is shown in Fig. 3 where it can be seen that there is little difference in maximum density between the three compositions chosen although it does appear that the temperature of maximum densification varies with composition. Composition 1 has a maximum density at about 1550°C, composition 2 at 1530°C and in the case of composition 3 the maximum density occurs at a lower temperature (around 1500°C or lower). The difference in behaviour can be ascribed to the different amounts of liquid phase present in the compositions and in the phases formed. Compositions 1 and 2 are in the same phase field ($O' + X + \text{liquid}$) with the first composition closer to the binary solid

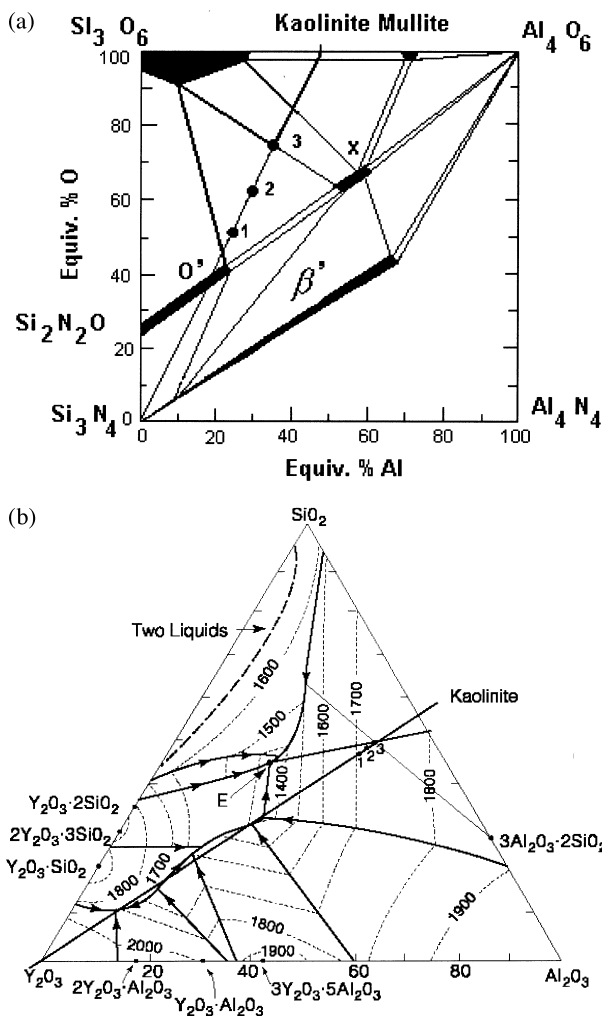


Fig. 2. Phase diagrams (a) $\text{Si}_3\text{N}_4\text{-SiO}_2\text{-Al}_2\text{O}_3\text{-AlN}$, and (b) $\text{SiO}_2\text{-Al}_2\text{O}_3\text{-Y}_2\text{O}_3$.

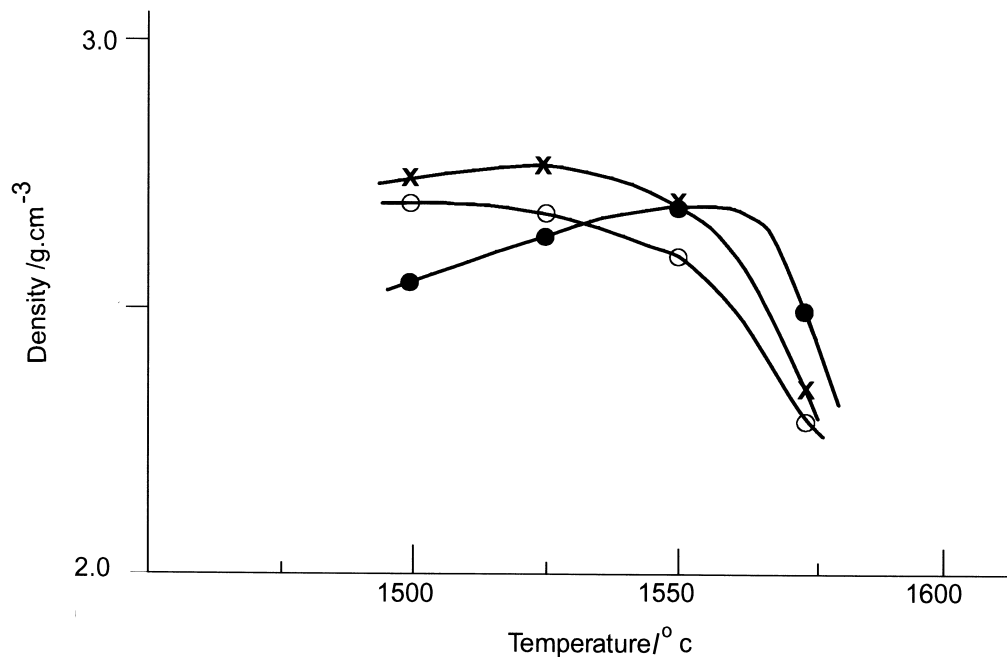


Fig. 3. Density as a function of sintering temperature for the matrix compositions 1 (—●—), 2 (—×—) and 3 (—○—).

edge of the phase field and therefore likely to produce less liquid for sintering which is consistent with the lower density curve for this sample at lower temperatures than for composition 2 (as shown in Fig. 3). Composition 3 is also in the ($O' + X + \text{liquid}$) field with a higher liquid proportion than for either of the other samples and close to the binary edge of liquid + X. In this case the higher density at lowest temperatures (1500°C) is followed by a rapid decrease in density with temperature which is accompanied by pronounced swelling of the samples due to excessive liquid phase formation. This latter effect is noticeable in all three compositions when sintered at 1580°C . The phases present in all three compositions were determined by X-ray diffraction after cooling from sintering temperature. The evolution of the phase distributions are shown in Table 1.

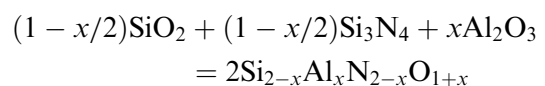
For each composition sintered at 1500°C for 4 h the main crystalline phases are silicon oxynitride solid solution (O') and mullite (A_3S_2) but the relative proportions vary with composition. Composition 3 has the highest oxide content, is closest to the binary oxide edge of the phase field and has the highest proportion of mullite (60 at% 1500°C). The oxide liquid phase, which forms in the first stage of sintering, promotes the chemical reactions which take place during sintering and leads to precipitation of mullite from the liquid phase. Decomposition of kaolinite (from clay) on heating yields, successively, metakaolin and crystallisation of mullite with rejection of silica;



Table 1. X-ray diffraction data for matrix mixes

Composition number	Temperature ($^{\circ}\text{C}$)	Phase identification	Phase percentages
1	1500	$O' A_3S_2$	67:33
1	1530	$O' X, A_3S_2$	67:25:8
1	1550	O', X	67:33
2	1500	O', A_3S_2	60:40
2	1530	O', A_3S_2, X	50:25:25
2	1550	O', X	60:40
3	1500	A_3S_2, O'	60:40
3	1530	O', A_3S_2, X	45:45:10
3	1550	X, O', A_3S_2	50:33:17

Reaction of the silicon nitride in the formulations with the liquid phase then leads to precipitation of O' which can be shown as;



with the O' phase containing the maximum content of aluminium ($2x = 0.2$) as can be seen from Fig. 2(a). Yttrium is not found in O' or in mullite and is concentrated in the residual liquid phase which solidifies on cooling to form intergranular glass. As the sintering temperature increases, X-ray patterns show that the relative intensity of O' remains approximately constant, mullite decreases and that of X-phase increases. At 1530°C all three compositions contain three crystalline phases with the amount of mullite increasing from compositions

1 to 3 as would be expected from Fig. 2, and at 1550°C no mullite is detected by X-ray diffraction in compositions 1 and 2 but some remains in composition 3. In the latter composition the amount of O' is greater than expected from the phase diagrams and this together with the presence of mullite is found to be due to insufficient time for this composition to reach equilibrium. This is confirmed by the study of the composite samples described below.

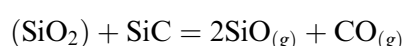
3.2 Densification and microstructural development of sialon-silicon carbide composites

From studies of the matrix batches alone, for all three compositions the optimum sintering temperature was taken as 1530°C with the phase distributions after the basic 4 h sintering cycle of (Table 1);

Composition 1	67% O' + 8% mullite + 25% X
Composition 2	50% O' + 25% mullite + 25% X
Composition 3	45% O' + 45% mullite + 10% X

Composites were then made up as described in the Experimental section and fired at 1530°C for 4, 8, and 16 h. Table 2 gives the physical characteristics of the fired composites.

The physical characteristics of the fired composites (Table 2) show that as sintering time increases all physical changes are small. The small weight losses are probably due to loss by decomposition of some silicon nitride at the surface of the samples and by volatilisation of SiO and CO from the reaction of silicon carbide with the oxide liquid phases,



where (SiO₂) represents silica at reduced activity in the liquid phase, but the limited extent of the weight loss indicates that there is practically no interfacial reaction between the matrix and reinforcement under most of these time and temperature conditions. This is confirmed by examination of the microstructures given below.

Shrinkage is due to the formation of O' and X phase from the liquid phase reaction and the extent of shrinkage is small because of the formation of a rigid skeleton of silicon carbide particles which adopt a lowest energy configuration but then resist (by particle contact) any further shrinkage in the composite. This is beyond the upper bound of the rule of mixtures model of composite sintering^{8,9} which assumes that there is no interparticle interaction. There is apparently some expansion of the composite during sintering in the case of composition A however this is within the accuracy of the measurement of sintering shrinkage.

Porosity is also relatively constant at 12% (±2%) but as is common in these systems is more variable than other measures of sintering due to the wide range of silicon carbide grit sizes used and the consequent variability from batch to batch in small processing runs.

X-ray diffraction examination of the products of reaction (Table 2) show that there is no mullite remaining in the crystalline phase assemblage of composites A and B which is consistent with the phase relations in Fig. 2(a) and the matrix phases in Table 1. It is also to be noted that to reach phase equilibrium higher temperature (Table 1) or longer time (Table 2) are required. The more reducing environment resulting from the incorporation of silicon carbide (compared to the matrix sinterings described above) and consequent incorporation of additional nitrogen from the gas atmosphere into the liquid phase will influence the final matrix compositions but the X-ray analysis is not sufficiently precise to determine these changes. The matrix composition remains in the phase field of the original powder composition. The final composition of composite C is however not consistent with the phase diagram as a relatively high proportion of O'-sialon remains in the final composition. It must be concluded therefore that the small reducing effect of the carbide (weight loss column in Table 2) has shifted the composition downwards and to the right in the phase diagram of Fig. 2(a) (loss of silicon and oxygen) to put the composition further into the (X + O' + liquid) field and away from the binary (liquid + X) boundary. This is consistent with previous observations.¹

Table 2. Characteristics of composites A, B and C (matrices 1, 2 and 3 containing 60% SiC)

Composites	Time (h)	Density (g)	Wt loss (%)	Porosity (%)	Shrinkage (%)	Phases (excluding SiC)
A	4	2.63	0.5	11	-1	O', X, A ₃ S ₂
A	8	2.58	0.6	14	-2	O', X
A	16	2.54	1.4	15	-3	O', X
B	4	2.70	1.0	11	1	O', X, A ₃ S ₂
B	8	2.67	1.4	12	1	O', X
B	16	2.61	2.9	13	0	O', X
C	4	2.71	1.0	10	1	O', X, A ₃ S ₂
C	8	2.69	1.7	11	1	X, O', A ₃ S ₂
C	16	2.61	4.0	12	0	X, O'

Optical microstructures of polished sections show that a good interface between the reinforcement and the matrix has been formed. Figures 4–6 show examples of the three composites in which the silicon carbide grains are evident and the matrix consists of a glassy continuum containing acicular precipitates of the oxynitride phases. The irregular shape of the original crushed/ground carbide is evident and confirms the weight loss data (Table 2)

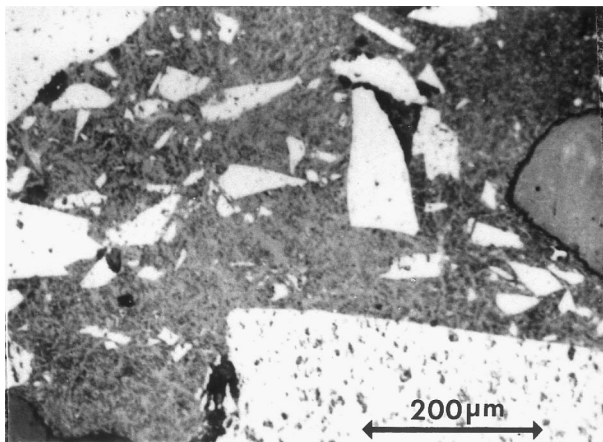


Fig. 4. Optical micrograph of composite A sintered at 1530°C for 16 h.

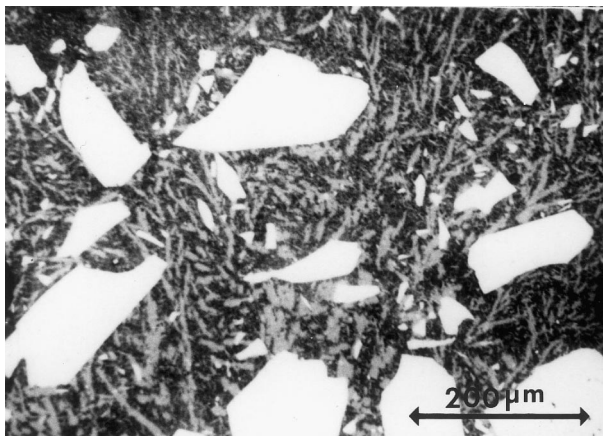


Fig. 5. Optical micrograph of composite B sintered at 1530°C for 16 h.

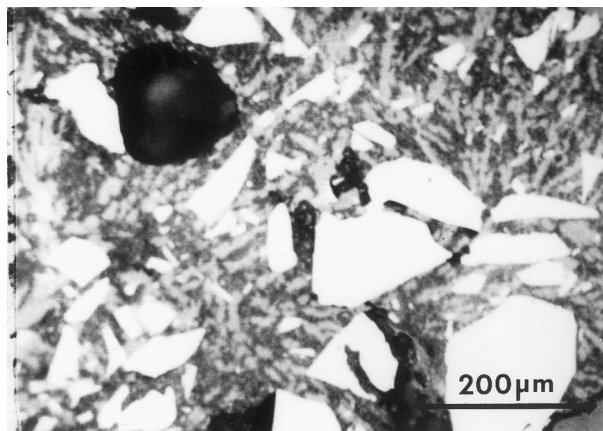


Fig. 6. Optical micrograph of composite C sintered at 1530°C for 16 h.

that no significant extent of interfacial reaction has occurred between the carbide and liquid phase at sintering temperature. Microanalysis of the metallic elements in the SEM show that the coarser, broader needles are X-phase and the finer distribution is O'. The difference between the latter phases is more obvious in SEM photographs of the fracture faces of broken samples shown in Figs 7–9. The rod-like shape of O' (Figs 7 and 8) is clearly seen as the finer (10 μm length and 1 μm diameter) of the two crystalline phases with X-phase forming considerably coarser, flatter laths (Fig. 9). These observations are consistent with the reported^{14,15} morphology and mechanisms of formation of O' from oxynitride liquids. Neither of the crystalline phases is known to accommodate yttrium and so it is assumed that it is all present in the glass (SEM microanalysis is inconclusive since the penetration depth of the beam is greater than the thickness of the precipitates and so a spot analysis gives information from both crystalline phase and surrounding glass).

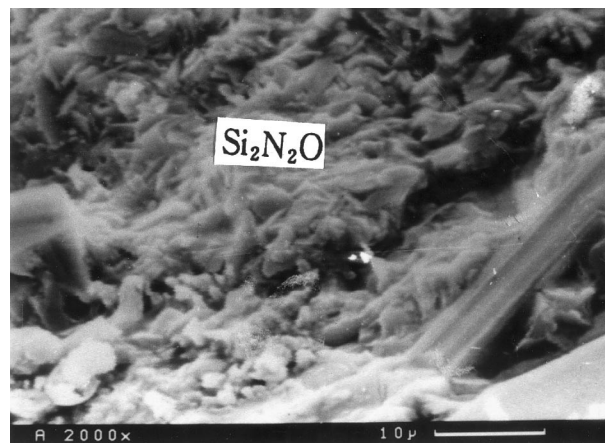


Fig. 7. SEM micrograph of the matrix in composite A fired at 1530°C for 16 h and showing the fine needle appearance of O' phase.

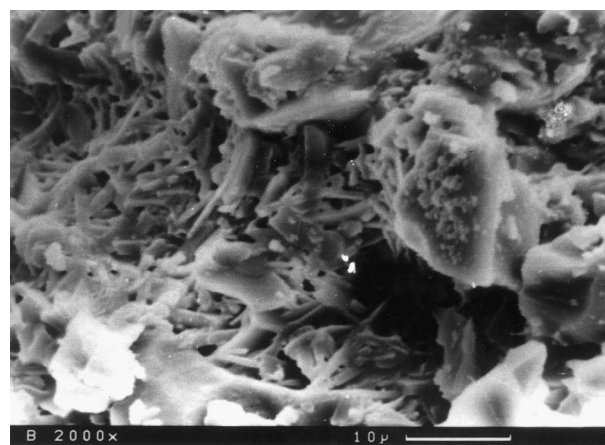


Fig. 8. SEM micrograph of a fracture surface showing the matrix in composite B with fine needles of O' phase (sintered at 1530°C for 16 h).

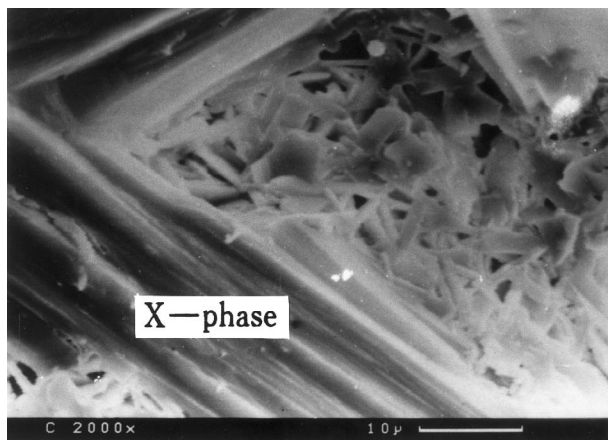


Fig. 9. SEM micrograph of a fracture surface in composite C showing laths of X-phase sialon after sintering at 1530°C for 16 h.

The presence of yttrium in the glass is known from the work of Drew *et al.*¹⁶ to increase the viscosity of the glass and therefore to have a strong effect on visco-plastic creep behaviour.¹² Similarly, it has been shown that tensile creep of silicon nitride is strongly influenced by the aspect ratio of the crystalline phases.¹⁷ Although the mechanical behaviour of the composites is not evaluated in this work, the microstructures were designed with these factors in view. Thus it is expected that the combined action of the silicon carbide reinforcement skeleton, the interlocking acicular crystalline phases and the high-temperature glass will offer the prospect of improved high-temperature properties. With respect to the other property requirements indicated in the Introduction, the 12% porosity (Table 2) is almost entirely closed and therefore the materials will have the required low gas permeability, and the linear shrinkage on sintering (Table 2) is sufficiently close to zero to provide the level of dimensional stability required for the tubular shapes in the chosen application shown in Fig. 1.

4 Conclusions

The results of this investigation show that the matrix which is formed from reaction of clay with silicon nitride in the presence of yttria as a sintering additive is effective in producing nitride-bonded silicon carbide with minimum linear shrinkage on densification and controlled porosity. The results indicate that the matrix is formed by a series of steps:

1. Decomposition of china clay and formation of mullite and silica on heating.
2. Formation of liquid phase from these reaction products, together with excess silica from silicon carbide and yttria sintering additive.

3. Dissolution of silicon nitride in the liquid and precipitation of X and O'.
4. Formation of a high-yttrium, nitrogen glass on cooling.

Composites of this kind with porosity of about 14% and zero linear shrinkage on firing are promising candidate materials for radiant heater burner tubes¹⁸ where the microstructure offers the prospect of superior high-temperature strength to that of calcium-based ceramics through the continuous interlocking texture of the X and O' crystalline phases, the higher viscosity yttrium–nitrogen glass matrix and the interlocking carbide reinforcement.

References

1. Edrees, H. J., Holling, G. E. and Hendry, A., Sialon bonding systems for silicon carbide composites. *Br. Ceramic Trans.*, 1995, **94**, 52.
2. Hampshire, S. and Jack, K. H., The kinetics of densification and phase transformation of nitrogen ceramics. In *Special Ceramics 7* (ed. D. Taylor and P. Popper) Br. Ceramic Proceedings, vol. 31, Institute of Ceramics, Stoke-on-Trent, 1981, p. 37.
3. Quackenbush, C. L., Smith, J. T., Nail, J. and French, K. W., Sintering properties and fabrication of $\text{Si}_3\text{N}_4\text{-Y}_2\text{O}_3$ based ceramics. In *Progress in Nitrogen Ceramics*, ed. F. L. Riley. Martinus Nijhoff, Leyden, The Netherlands, 1983, p. 669.
4. Jack, K. H., The crystal chemistry of the sialons and related nitrogen ceramics. In *Nitrogen Ceramics*, ed. F. L. Riley, Noordhof, Leyden, The Netherlands, 1977, 109.
5. Patel, J. K. and Thompson, D. P., The devitrification behaviour of grain-boundary glasses in silicon nitride with mixed magnesia–yttria additions. In *Engineering with Ceramics 2*, ed. R. W. Davide, Br. Ceramic Proceedings, Vol. 39, Institute of Ceramics, Stoke-on-Trent, 1987, 72.
6. Edrees, H. J. and Hendry, A., Pressureless sintering of pre-prepared sialon powders. In *Complex Microstructures*, ed. R. Stevens and D. Taylor, Br. Ceramic Proceedings, Vol. 42, Institute of Ceramics, Stoke-on-Trent, 1989, 49.
7. Grathwohl, G., Hanna, S. B. and Thummler, F., Hot pressing and properties of silicon nitride powder. *Br. Ceramic Trans.*, 1982, **81**, 193.
8. Edrees, H. J., Smith, A. C. and Hendry, A., A rule-of-mixtures model for sintering of particle-reinforced ceramic-matrix composites. *J. Eur. Ceram. Soc.*, 1998, **18**, 275.
9. Edrees, H. J. and Hendry, A., Shrinkage and densification of particulate reinforced ceramic-matrix composites. *Br. Ceramic Trans.*, **98**, 1999, 1.
10. Das, P. K. and Mukerji, P. C., Sintering behaviour and properties of Si_3N_4 sintered with nitrogen-rich liquid in the $\text{Y}_2\text{O}_3\text{-AlN-SiO}_2$ system. *Adv. Ceramic Materials*, 1988, **3**, 234.
11. Levins, E. M., Robbins, C. R., McMurie, H. I. and Reser, M. K. (eds), *Phase Diagrams for Ceramists (Supplement)*. American Ceramic Society, Columbus, OH, 1969.
12. Descamps, P., Poorteman, M., Cambier, R., O'Sullivan, D., Courtois, C. and Leriche, A., Study of the creep behaviour of $\text{Al}_2\text{O}_3\text{-SiC}$ nanocomposites. In *Ceramic Composite Composites IV*, ed. A. Leriche, V. Lardot, D. Libert and I. Urbain. Belgian Ceramic Society, Mons, Belgium, 1997, p. 161.
13. Naik, I. K., Gauckler, L. J. and Tien, T. Y., Solid–liquid equilibria in the system $\text{Si}_3\text{N}_4\text{-AlN-SiO}_2\text{-Al}_2\text{O}_3$. *Am. Ceram. Soc.*, 1978, **61**, 332.

14. Bergman, B. and Heping, H., The influence of different oxides on the formation of $\text{Si}_2\text{N}_2\text{O}$ from SiO_2 and Si_3N_4 . *J. Eur. Ceram. Soc.*, 1990, **6**, 3.
15. Huang, Z. K., Griel, P. and Petzow, G., Formation of silicon oxynitride from Si_3N_4 and SiO_2 in the presence of Al_2O_3 . *Ceramics International*, 1984, **10**, 14.
16. Drew, R. A. L., Hampshire, S. and Jack, K. H., Nitrogen glasses. In *Special Ceramics 7*, ed. D. Taylor and P. Popper, Br. Ceramic Proceedings, vol. 31, Institute of Ceramics, Stoke-on-Trent, 1981, p. 119.
17. Ohji, T., Yamauchi, Y. and Kanzaki, S., Tensile creep and creep rupture behaviour of HIPed silicon nitride. In *Silicon Nitride 93*, eds. M. J. Hoffmann, P. F. Becher and G. Petzow, Trans Tech, Aedermansdorf, Switzerland, 1994, p. 569.
18. Mansfield, J., Holling G. E. and Hendry, A., Fibre reinforcement of CMC combustion tubes. In *Ceramic Ceramic Composites IV*, eds. A. Leriche, V. Lardot, D. Libert and I. Urbain, Belgian Ceramic Society Mons, Belgium, 1997, p. 137.